



SO₂ Layer Height retrieval from Sentinel-5 Precursor/TROPOMI using FP_ILM

Pascal Hedelt¹, Dmitry S. Efremenko¹, Diego G. Loyola¹, Robert Spurr², and Lieven Clarisse³

¹Remote Sensing Technology institute (IMF), German Aerospace Center (DLR), Oberpfaffenhofen, Germany

²RT Solutions Inc., Cambridge, MA, USA

³Université libre de Bruxelles (ULB), Service de Chimie Quantique et Photophysique, Atmospheric Spectroscopy, Brussels, Belgium

Correspondence: P. Hedelt (pascal.hedelt@dlr.de)

Abstract. Accurate determination of the location, height and loading of SO₂ plumes emitted by volcanic eruptions is essential for aviation safety. The SO₂ layer height is furthermore one of the most critical parameters that determine the impact on the climate. Retrievals of SO₂ plume height have been carried out using satellite UV backscatter measurements, but until now, such algorithms are very time-consuming. We have developed an extremely fast yet accurate SO₂ layer height retrieval using the Full-Physics Inverse Learning Machine (FP_ILM) algorithm. This is the first time the algorithm has been applied to measurements from the TROPOMI instrument on board the Sentinel-5 Precursor platform. In this paper, we demonstrate the ability of the FP_ILM algorithm to retrieve SO₂ plume layer heights in near-real-time applications with an accuracy of better than 2 km for SO₂ total columns larger than 20 DU. We present SO₂ layer height results for a selection of recent volcanic eruptions observed by TROPOMI.

10 *Copyright statement.*

1 Introduction

Global satellite observations allow for the timely detection and monitoring of SO₂ emitted from volcanic eruptions, even in remote regions, where no ground-based instruments are installed (see e.g. Fioletov et al. 2013). Satellite measurements of UV earthshine spectra in the wavelength range between 305 and 335 nm provide the highest sensitivity to SO₂ in the Earth's atmosphere. Volcanic eruptions can inject large amounts of sulphur dioxide (SO₂) into the atmosphere, where it is either subject to dry and wet deposition within a few days in the troposphere (see e.g. Lee et al. 2011 or Myles et al. 2011), or oxidization over a period of several weeks to sulfate aerosols in the stratosphere (see e.g. Robock, 2000; Forster et al., 2007 and von Glasow et al. 2009). Sulfate aerosols can affect the Earth's radiative forcing and have an impact on clouds (see e.g. McCormick et al., 1995; Robock, 2000 and Malavelle et al. 2017).

20 Based on UV earthshine measurements, SO₂ vertical column densities (VCDs) can be retrieved easily using for example the Differential Optical Absorption Spectroscopy (DOAS) algorithm, see e.g. Rix et al. (2012), or the Principal Component



Analysis (PCA) algorithm, see e.g. Li et al. (2017). These methods are fast enough for near-real-time (NRT) retrievals. Nevertheless, both DOAS and PCA algorithms retrieve only the slant column - in order to calculate the VCD, explicit or implicit assumptions about the vertical distribution of SO₂ have to be made in order to determine the effective light path - this VCD conversion factor is called the airmass factor (AMF). In the UV range between 305 - 335 nm, AMFs are calculated by means of multiple-scattering radiative transfer models assuming known vertical distributions of SO₂ and O₃.

However, the SO₂ VCD is strongly dependent on the vertical distribution (in terms of the plume layer height) of SO₂, a quantity which is usually unknown at the time of the measurement. Even if there are ground-based or aircraft measurements of the SO₂ layer-height (LH), the data are generally difficult to use for validation, since e.g. for strong eruptions, volcanic plumes are typically transported over long distances and the number of collocations is small. Thus, for volcanic SO₂ measurements, the vertical distribution of SO₂ is a key parameter limiting the product accuracy.

The determination of the vertical distribution of SO₂ based on satellite data is however challenging, since the information about the vertical distribution is not easy to extract from the spectral signature (see Yang et al. 2009 and Nowlan et al. 2011). The SO₂ loading (VCD) has a direct effect on the optical depth, whereas the layer height (LH) has an indirect effect on the optical depth since it influences both the number of photons passing through the SO₂ layer as well as the layer optical depth due to the temperature dependency of the SO₂ absorption crosssections (Yang et al., 2009).

In the operational Sentinel-5 Precursor/TROPOMI product (see Theys et al. 2017), the SO₂ VCDs are hence provided for a set of a priori SO₂ distributions, along with an averaging kernel (AK), in order that the user can calculate the VCD for an arbitrary SO₂ vertical distribution.

To date, SO₂ layer-height retrievals have used computationally demanding direct fitting inversion methods, which are not suitable for NRT applications. For the retrievals based on satellite UV measurements, Yang et al. (2009) and Yang et al. (2010) developed an Extensive Iterative Spectral Fitting (EISF) algorithm for OMI, and Nowlan et al. (2011) introduced an optimal estimation (OE) scheme for GOME-2. For strong volcanic eruptions, the accuracy of the retrieved SO₂ LH using this approach is in the range 0.5–1 km, whereas for small SO₂ absorption it is around 2 km (see Nowlan et al. 2011).

Satellite infrared sounders also offer the opportunity to measure both SO₂ VCDs and LH (see Clarisse et al., 2008; Carboni et al., 2012; Clarisse et al., 2014 and Carboni et al. 2016) using optimal estimation algorithms for IASI. While infrared sounders have a weaker sensitivity to the lower tropospheric SO₂ than UV instruments, the layer height retrievals tend to have a better accuracy, and perform well even for low column amounts (up to the DU-level), however at a low horizontal resolution of about 12 km.

In contrast, the TROPOMI instrument, on board the Sentinel-5 Precursor satellite (S5P) launched on 13 October 2017, has a much higher spatial resolution of $7 \times 3.5 \text{ km}^2$, with the possibility of operation at an even smaller resolution of $5.5 \times 3.5 \text{ km}^2$. This allows us to observe and study SO₂ plumes at an unprecedented level of detail. Data turnover from TROPOMI is very large, and this consideration will require the development of new retrieval schemes for the fast and accurate retrieval of SO₂ layer heights in an operational environment.

To this end, we have developed an algorithm called 'Full-Physics Inverse Learning Machine' (hereafter referred to as FP_ILM) for the retrieval of the SO₂ LH based on satellite UV earthshine spectra. The FP_ILM algorithm has been used



for the retrieval of ozone profile shapes (Xu et al., 2017), the retrieval of surface properties accounting for the BRDF effects (Loyola et al., 2019), and the retrieval of SO₂ LH from GOME-2 (Efremenko et al., 2017). The algorithm creates a mapping between the spectral radiance and SO₂ LH using machine learning methods. The time-consuming training phase of the algorithm using radiative transfer model calculations is performed off-line, and only the inversion operator has to be applied to satellite
5 measurements - this makes the algorithm extremely fast and it can thus be used in near-real time processing environments. In this second paper on the FP_ILM SO₂ LH, we describe some improvements to the algorithm, and we apply it to a number of volcanic eruptions observed by TROPOMI during the commissioning phase (started 7 November 2017) as well as the first operational phase (started April 2018).

The paper is organized as follows: In Section 2 we describe the improved FP_ILM SO₂ LH algorithm. The sensitivity of
10 retrieved SO₂ LHs to a number of different parameters is discussed in Section 3. In Section 4, the FP_ILM is applied to S5P data to retrieve SO₂ LHs for selected volcanic eruptions. We summarize the paper in Section 5.

2 FP_ILM algorithm

Conceptually, the FP_ILM consists of a training phase, in which the inversion operator is obtained using synthetic data generated with an appropriate radiative transfer (RT) model, and an operational phase, in which the inversion operator is
15 applied to real satellite measurements. The main advantage of the FP_ILM over classical direct fitting approaches is that the time-consuming training phase involving complex RT modeling is performed offline; the inverse operator itself is robust and computationally simple and therefore extremely fast.

During the training phase, the Linearized Discrete Ordinate Radiative Transfer model (LIDORT) with inelastic rotational Raman scattering (RRS) implementation (Spurr et al., 2008) is deployed to compute simulated reflectance spectra in the
20 wavelength range 310 – 335 nm. These spectra depend upon the following $n = 8$ input parameters: the SO₂ VCD and LH, the surface albedo, the surface height, the O₃ VCD, the solar zenith angle (SZA), the viewing zenith angle (VZA) and the relative azimuth angle (RAA). Table 1 gives a summary of the parameter space. O₃ profiles are classified according to the total column amount of ozone, and the month and latitude zones as specified in the TOMS Version 8 O₃ profile climatology (Bhartia, 2003). The SO₂ profile plume is taken to have a Gaussian shape, characterized by the total SO₂ VCD loading and centered at a peak-
25 concentration layer height z_p , along with a half-width fixed to 2.5 km. In the following, the retrieval of SO₂ layer height refers to the retrieval of the peak-concentration height z_p .

Simulations were done on a pressure/temperature/height grid from the US standard atmosphere, with a finer-grid vertical height resolution of 0.25 km below 15 km in order to resolve properly the Gaussian SO₂ plume shape. In total, some 131,072 simulated reflectance spectra have been calculated on a selective parameter grid established by means of a smart sampling
30 technique developed by Loyola et al. (2016).

The use of the LIDORT-RRS RT model is necessary, as it enables us to account for the effect of Raman scattering in the atmosphere. Solar irradiances exhibit strong Fraunhofer structures in this part of the UV spectral range, and earthshine spectra are characterized by the "filling-in" of Fraunhofer-solar and telluric-absorber features due to "inelastic" (wavelength-



redistributed) rotational-Raman scattering by air molecules. For further details, see Efremenko et al. (2017) and Spurr et al. (2008).

The simulated high-resolution reflectance spectra are then convolved with the TROPOMI Instrument Spectral Response Functions (ISRF) v3.0.0 (released 2018-04-01)¹. Note that the TROPOMI instrument comprises 450 rows, which are in principle single detectors with their own ISRFs. The signal-to-noise ratio (SNR) is about 1000 in our UV wavelength range. Thus, to account for instrumental noise in the training phase, uncorrelated Gaussian noise with a fixed SNR of 1000 is added to the simulated spectral data.

To extract the information about the layer height and to reduce the dimensionality of the spectral dataset, a principal components analysis (PCA) is applied to the simulated spectra. By thus characterizing the set of simulated measurements with fewer parameters, a simpler, more stable and computationally efficient inversion scheme can be realized. It was found that using 10 principal components (PCs) is sufficient to retrieve information about the layer-height. The inclusion of additional PCs beyond 10 did not result in any improvements to LH retrievals, since higher-order PCs are increasingly affected by noise. Figure 6 shows the ratio between the variance of the PCA-derived data set and the total variance of the complete spectra data set (the "explained" variance ratio) as a function of number of PCs included in the PCA. Already with 10 PCs, the error is less than 1×10^{-4} .

The dimensionality-reduced training spectra, together with the information about the O₃ VCD, the SZA/VZA/RAA angles, and the surface pressure and albedo, are then used as input to train a feed-forward artificial neural network (MultiLayer Perceptron Regression - MLPR), with the SO₂ LH as the output layer. Note here that the SO₂ VCD is not part of the training, since it depends directly on the SO₂ layer height. The training of the MLPR is an iterative process; at each time step, the partial derivatives of the loss function with respect to the model parameters are computed in order to update the parameters. A regularization term is added to the loss function that shrinks model parameters to prevent over-fitting: By building a complex neural network, it is quite easy to perfectly fit the training dataset. When this model is however evaluated on new data (here satellite measurements), it performs very poorly. The regularization modifies the loss function by adding additional terms that penalize large weight vectors and preferring diffuse weight vectors.

After carrying out a PCA and MLPR parameter optimization using closed-loop retrievals to minimize differences between the retrieved and simulated layer heights, the final configuration for the neural network settled on the use of two hidden layers, with 32 nodes in the first layer and 10 nodes in the second.

In the operational phase, the first step is to use the principal component scores acquired during the training phase to transform a given TROPOMI spectral measurement data set to one with a lower dimension. Once this is done, the neural network inverse function is then applied to retrieve the SO₂ LH.

¹ Available here:

<http://www.tropomi.eu/data-products/isrf-dataset/>



3 Dependencies

In this section, we study the dependency of the layer height retrieval on different parameters. We discriminate between direct (i.e. those parameters affecting the reflectance spectra) and indirect (i.e. affecting the training data and inversion algorithm) dependencies of the retrieved layer height.

- 5 – Direct dependencies: Viewing geometry, surface properties, ISRF, Noise level (SNR)
- Indirect dependencies: Number of layers in the neural network, number of PCs, parameter ranges for training

To proceed, we first divide the training dataset, using 90% of the data for training of the inversion operator and the remaining 10% for testing. Furthermore, we have generated an independent verification dataset modeled with LIDORT_RRS for selected input parameters on a prescribed parameter grid with fixed layer heights of 2.5, 6.5, 13 and 20 km. This verification dataset
10 thus differs from the training dataset, where a "smart" parameter grid was used in place of fixed parameter values.

First, we train the FP_ILM operator using 90% of the training dataset (see Table 1), and then apply the trained operator to the remaining 10% training spectra, for which we know the exact SO₂ LH. Figure 1 shows the SO₂ LH difference as a function of solar/viewing geometry, SO₂ VCD, O₃ VCD, albedo and surface pressure. The figure shows clearly a number of marked dependencies in the retrieved layer height, with notably high differences with respect to the real SO₂ LH for low and high layer
15 heights, for low SO₂ VCD well as for high SZA.

Regarding the SZA dependency, a cutoff limit of 75° is set in operational SO₂ retrievals, because at high SZA the light path becomes very long and the noise level increases. Accordingly, we limit the SZA of the spectra used in the training to SZA < 70° in the following.

Clearly, for small SO₂ VCDs, the information content on LH in the spectral signature is very low. It follows that the inclusion
20 of spectra with low SO₂ content in the training will have a negative effect on the entire neural network. In principle for lower SO₂ VCD loadings, more PCs could be included, but at some point also the noise level signature will exceed that of the actual SO₂ absorption.

We have performed several tests in which we limit the training dataset by varying the allowed input parameter ranges. We have finally found an optimal parameter range that allows the retrieval of a broad range of SO₂ LHs even for low SO₂ VCDs. In
25 the training phase, we use only spectra with SO₂ VCD > 20 DU, surface albedo < 0.5 and SZA < 70° to train the final inversion operator for TROPOMI. Figure 2 shows that the error on the retrieved SO₂ LH is less than 2 km and the dependency on SO₂ VCD is reduced.

In addition, we have applied the optimized FP_ILM operator to the independent verification dataset with its prescribed SO₂ LHs. Figure 3 shows the retrieved layer height as a function of SO₂ VCD. As mentioned above, for low SO₂ VCDs, high-
30 altitude layer heights cannot be retrieved - there is always a bias towards low layer heights. Only for SO₂ loadings in excess of 20 DU, do we retrieve layer heights with an uncertainty of less than 2 km.



To investigate the dependency of the retrieved SO₂ LH as a function of SNR, we have added noise (SNR of 800, 1000 and 1200) to the independent verification spectra. Figure 4 clearly shows that the accuracy of the retrieved layer height improves with increasing SNR.

In the operational retrieval of SO₂ LHs from TROPOMI data, each detector row is effectively a single instrument with its own ISRF. The accuracy of the retrieved SO₂ LH can vary across detector rows. Figure 5 shows the SO₂ LH results when applied to the Sinabung eruption (see Section 4.2). Black dots show the LH for each 50th row, whereas the red cross shows the interpolated LH for the measurement row. Clearly, the retrieved LH is slightly different in each row (within 1 km) due to the different ISRF used for training the NN. Note that in the final operational retrieval, we determine the layer height for a set of fixed detector rows (for which we have trained the FP_ILM separately), and then interpolate the layer height to the actual row. In this way we avoid jumps in the retrieved layer height between adjacent detector rows.

4 Application to TROPOMI data

Reflectance spectra from TROPOMI are determined from the L1 solar irradiance and earthshine radiance data (solar irradiance is measured on a daily basis). To correct for Doppler shifts between earthshine and irradiance spectra, we apply the wavelength calibration information from the operational L2 SO₂ product to first calibrate the solar spectrum and then we use the fitted shift and squeeze parameters from the DOAS retrieval to calibrate the earthshine spectra. From this calibrated L1 data, we then calculate reflectances in the wavelength range 310 – 335 nm.

In the following subsections, we have applied the FP_ILM operator to a set of eight major volcanic eruptions measured by TROPOMI. We note that the SO₂ LH retrieval only takes about 2 ms per TROPOMI spectrum, hence even for an extended volcanic plume, the entire LH retrieval can be performed in a matter of seconds, which is important for operational retrieval environments with strong time constraints. To attempt validation of our results, we have performed comparisons with independent MetOp/IASI SO₂ LH data (see Clarisse et al. 2014 for details). The MetOp platforms are on completely different orbits from that of S5P, with widely different overpass times, so that direct satellite comparisons will give only a qualitative validation on the accuracy of retrieved SO₂ LHs from TROPOMI measurements. At the time of writing, IASI data is unfortunately the only source for independent satellite results.

4.1 Ambae

A few weeks after the start of the TROPOMI commissioning phase, strong volcanic activity was observed from the Ambae shield volcano (Vanuatu islands). Figure 7 (left) shows the SO₂ VCD retrieved by the standard operational SO₂ algorithm (Theys et al., 2017). We have applied the FP_ILM algorithm to TROPOMI measurements on two occasions (23 November 2017 as well as on 27 July 2018) for overpass times around 02:00h UTC.

On 23 November 2017, two plumes are clearly visible. The first is an aged plume traveling in a south-westerly direction, having a maximum SO₂ VCD of up to 77 DU and a LH of about 10–12 km, while the second plume is moving in a south-easterly direction with SO₂ LH of about 15 km (see Fig. 7). Figure 8 shows the SO₂ LH retrieved for IASI/MetOp-A and -B



measurements at overpass times around 11:00h and 21:00h, both events occurring well after the TROPOMI measurements in Fig. 7. Although this timing mis-match makes verification of the SO₂ LH difficult (the plume has already dispersed at the times of the IASI measurements), the maximum SO₂ LH is still about 12-14 km (with a maximum of 20 km), which is in agreement with the FP_ILM results for TROPOMI. The IASI SO₂ LH for the aged plume travelling in the south-west direction is however well below the 10 km LH retrieved by the FP_ILM.

On 27 July 2018 a thick SO₂ plume of up to 120 DU was observed, traveling eastwards, see Fig. 9. The retrieved SO₂ LH reached up to 20 km, into the stratosphere, where SO₂ lifetimes are very much longer - here it can form sulfate aerosols and acid rain within weeks. Figure 10 shows the respective IASI SO₂ LH results for overpass times around 13:00h and 23:00h UTC, respectively. The IASI SO₂ LH also peaks at around 20 km, hence showing a very good agreement with the FP_ILM LH results, although the plume has already dispersed.

4.2 Sinabung

On 19 February 2018, the Sinabung stratovolcano on the island of Sumatra erupted violently, with a volcanic plume containing ash and up to 50 DU of SO₂. The FP_ILM algorithm was applied to TROPOMI measurements with an overpass time of about 06:30h UTC. The retrieved SO₂ LH extends up to 17 km, see Fig. 11. For this eruption, there was also a NASA A-train overpass (at about 07:15h UTC) of the CALIOP/CALIPSO LIDAR instrument, with associated measurements clearly showing an attenuation by ash or aerosols at an altitude around 15-18 km (see Fig. 12); this is in excellent agreement with our FP_ILM results (see black diamonds in the figure). Figure 13 shows the corresponding SO₂ LH retrieved for IASI/MetOp-A and -B measurements with LH values at about 13 km for the 03:30h UTC overpass and LH up to 18 km around the overpass time of 15:00h UTC; these agree well with the TROPOMI results. Also the Pusat Vulkanologi dan Mitigasi Bencana Geologi² (PVMBG, also known as CVGHM) reported at 08:53h UTC *a dark gray plume with a high volume of ash that rose at least to 16.8 km*. Furthermore the Darwin Volcanic Ash Advisory Center³ (VAAC) reported that LH values for these Sinabung ash plumes were identified in satellite images, recorded by webcams, and reported by PVMBG continued to rise throughout the day to 13.7 km.

4.3 Sierra Negra

On 26 June 2018 a strong eruption at the Sierra Negra shield volcano located on Isabela Island (Galapagos) occurred. This eruption occurred in two phases, with an initial very energetic eruption characterized by the opening of five fissures and lava flows, followed by a second event which lasted until 23 August 2018 with decreased gas emissions. TROPOMI was able to measure a very strong SO₂ plume (with loading in excess of 500 DU) only a few minutes after the start of the first eruption. Figure 14 shows the strong and extended SO₂ plume on the 27 and 28th of June at an overpass time around 19:50h UTC, along with the SO₂ LH retrieved by the FP_ILM algorithm. Retrieved SO₂ LH values of about 14 km were observed, with some parts of the plume reaching about 18 km altitude. This is in good agreement with SO₂ LH retrieved from IASI data (see Fig.

²see <http://vsi.esdm.go.id/>

³see <http://www.bom.gov.au/aviation/volcanic-ash/>



15), even though the IASI measurements were taken at overpass times of 02:00h and 14:00h UTC (both well before the S5P overpass).

5 Conclusions

We have developed a new algorithm for the fast and accurate retrieval of SO₂ layer heights from UV earthshine observations of volcanic SO₂ eruptions by the TROPOMI sensor on board the Sentinel-5 Precursor platform. The SO₂ LH retrieval has two phases - (1) a computationally expensive off-line training phase in which the retrieval inverse operator is obtained using the FP_ILM (Full Physics Learning Machine) algorithm; and (2) a very fast operational phase, in which the FP_ILM inverse operator is applied to measured UV reflectance spectra. The FP_ILM combines a Principal Component Analysis with a Neural Network regression using the UV reflectance, O₃ total column, viewing geometries and surface properties as input. Based on an optimized training dataset created with smart sampling techniques, the principal component scores calculated for reflectance spectra in the wavelength range 310-335 nm are used along with the other parameters to train a feed-forward artificial neural network. For S5P/TROPOMI measurement data, an initial dimensionality reduction of the reflectance spectra is performed by applying the PCA-derived Principal Component scores before retrieving SO₂ LH with the trained Neural Network .

The FP_ILM can be used for NRT applications with strict time constraints. S5P/TROPOMI, with its high spatial and spectral resolution, provides a huge amount of data and the computationally intensive direct fitting approaches to SO₂ LH retrieval developed so far are not applicable. In contrast, the FP_ILM operator performs SO₂ LH retrieval within about 2 ms per TROPOMI spectrum. Hence even the retrieval on extended volcanic plumes can be performed in a matter of few seconds, allowing for the determination of the SO₂ layer height with an accuracy better than 2 km for SO₂ total column densities larger than 20 DU.

In this paper, we deployed an independent simulated reflectance spectra dataset to investigate the accuracy of SO₂ LH retrievals and their dependencies on a number of different factors and parameters both direct and indirect. In particular, it was found that retrieved SO₂ LH is strongly dependent on the SO₂ VCD for low VCDs <20 DU as well as for high SZAs >75°. For high VCDs and low SZA, the SO₂ LH can be retrieved with an accuracy of better than 2 km. We also investigated the dependencies on ISRF and SNR, both of which turned out to be relatively slight effects.

Broad-band spectral scattering and absorption due to sulfate aerosols or volcanic ash plumes will certainly affect SO₂ LH retrievals. Although not considered in the present work, we will address this important issue in a forthcoming paper in this series; aerosols will be accounted for explicitly in the training of the FP_ILM. Nevertheless, we should note that SO₂ and ash are likely to be collocated only for fresh volcanic plumes. For mature plumes, mass differences will ensure that ash and SO₂ plumes are not located at similar altitudes, and the corresponding plumes are thus subject to different wind-direction dispersal.

We have applied the FP_ILM to a number of strong volcanic eruptions observed recently by S5P/TROPOMI. Our SO₂ LH results have been compared to SO₂ LHs retrieved from IR measurements from two MetOp/IASI satellites. Unfortunately the orbits of both MetOp satellites and S5P have widely different overpass times, allowing only for qualitative comparisons. Despite this, there is in general a very good agreement between the IASI and TROPOMI results. In this regard, further verification work is certainly needed. For the Sinabung eruption in February 2018, our results were compared directly to CALIOP/CALIPSO



LIDAR data from an overpass right over the volcanic plume less than one hour after the S5P measurements. Our SO₂ LH was in excellent agreement with the 532 nm total attenuated LIDAR backscatter result, showing a volcanic plume peaking at around 18 km.

Acknowledgements. We are grateful to Nicolas Theys for helpful discussions of the SO₂ layer height retrieval from UV sensors. We hereby
5 acknowledge financial support from DLR programmatic (S5P KTR 2472046) for the development of TROPOMI retrieval algorithms. L.C.
is a research associate supported by the Belgian F.R.S.-FNRS.



References

- Bhartia, P.: Algorithm Theoretical Baseline Document, TOMS v8 Total ozone algorithm, Tech. rep., NASA, Greenbelt, Md., http://toms.gsfc.nasa.gov/version8/version8_update.html, 2003.
- Carboni, E., Grainger, R., Walker, J., Dudhia, A., and Siddans, R.: A new scheme for sulphur dioxide retrieval from IASI measurements: application to the Eyjafjallajökull eruption of April and May 2010, *Atmospheric Chemistry and Physics*, 12, 11 417–11 434, <https://doi.org/10.5194/acp-12-11417-2012>, <https://www.atmos-chem-phys.net/12/11417/2012/>, 2012.
- Carboni, E., Grainger, R. G., Mather, T. A., Pyle, D. M., Thomas, G. E., Siddans, R., Smith, A. J. A., Dudhia, A., Koukouli, M. E., and Balis, D.: The vertical distribution of volcanic SO₂ plumes measured by IASI, *Atmospheric Chemistry and Physics*, 16, 4343–4367, <https://doi.org/10.5194/acp-16-4343-2016>, <https://www.atmos-chem-phys.net/16/4343/2016/>, 2016.
- 10 Clarisse, L., Coheur, P. F., Prata, A. J., Hurtmans, D., Razavi, A., Phulpin, T., Hadji-Lazaro, J., and Clerbaux, C.: Tracking and quantifying volcanic SO₂ with IASI, the September 2007 eruption at Jebel at Tair, *Atmospheric Chemistry & Physics*, 8, 7723–7734, 2008.
- Clarisse, L., Coheur, P.-F., Theys, N., Hurtmans, D., and Clerbaux, C.: The 2011 Nabro eruption, a SO₂ plume height analysis using IASI measurements, *Atmospheric Chemistry & Physics*, 14, 3095–3111, <https://doi.org/10.5194/acp-14-3095-2014>, 2014.
- Efremenko, D. S., Loyola R., D. G., Hedelt, P., and Spurr, R. J. D.: Volcanic SO₂ plume height retrieval from UV sensors using a full-physics inverse learning machine algorithm, *International Journal of Remote Sensing*, 38, 1–27, <https://doi.org/10.1080/01431161.2017.1348644>, 2017.
- Fioletov, V. E., McLinden, C. A., Krotkov, N., Yang, K., Loyola, D. G., Valks, P., Theys, N., Van Roozendaal, M., Nowlan, C. R., Chance, K., Liu, X., Lee, C., and Martin, R. V.: Application of OMI, SCIAMACHY, and GOME-2 satellite SO₂ retrievals for detection of large emission sources, *Journal of Geophysical Research: Atmospheres*, 118, 11,399–11,418, <https://doi.org/10.1002/jgrd.50826>, <http://dx.doi.org/10.1002/jgrd.50826>, 2013JD019967, 2013.
- 20 Forster, P., Ramaswamy, V., Artaxo, P., Berntsen, J., Betts, R., Fahey, D. W., Haywood, J., Lean, J., Lowe, D. C., Myhre, G., Nganga, J., Prinn, R., Raga, G., Schulz, M., van Dorland, R., Bodeker, G., Boucher, O., Collins, W. D., Conway, T. J., Dlugokencky, E., Elkins, J. W., Etheridge, D., Foukal, P., Fraser, P., Geller, M., Joos, F., Keeling, C. D., Keeling, R., Kinne, S., Lassey, K., Lohmann, U., Manning, A. C., Montzka, S. A., Oram, D., O’Shaughnessy, K., Piper, S. C., Plattner, G. K., Ponater, M., Ramankutty, N., Reid, G. C., Rind, D., Rosenlof, K. H., Sausen, R., Schwarzkopf, D., Solanki, S. K., Stenchikov, G., Stuber, N., Takemura, T., Textor, C., Wang, R., Weiss, R., and Whorf, T.: Changes in atmospheric constituents and in radiative forcing, chap. 2, pp. 129–234, Cambridge University Press, Cambridge; New York, n/a, 2007.
- Lee, C., Martin, R. V., van Donkelaar, A., Lee, H., Dickerson, R. R., Hains, J. C., Krotkov, N., Richter, A., Vinnikov, K., and Schwab, J. J.: SO₂ emissions and lifetimes: Estimates from inverse modeling using in situ and global, space-based (SCIAMACHY and OMI) observations, *Journal of Geophysical Research: Atmospheres*, 116, n/a–n/a, <https://doi.org/10.1029/2010JD014758>, <http://dx.doi.org/10.1029/2010JD014758>, d06304, 2011.
- 30 Li, C., Krotkov, N. A., Carn, S., Zhang, Y., Spurr, R. J. D., and Joiner, J.: New-generation NASA Aura Ozone Monitoring Instrument (OMI) volcanic SO₂ dataset: algorithm description, initial results, and continuation with the Suomi-NPP Ozone Mapping and Profiler Suite (OMPS), *Atmospheric Measurement Techniques*, 10, 445–458, <https://doi.org/10.5194/amt-10-445-2017>, <https://www.atmos-meas-tech.net/10/445/2017/>, 2017.
- 35 Loyola, D., Xu, J. Heue, K. P., and Zimmer, W.: Applying FP_ILM to the retrieval of effective Lambertian equivalent reflectivity to account for BRDF effects on satellite UV/VIS trace gas measurements, submitted to Atmos. Meas. Tech., pp. 35–40, 2019.



- Loyola, D. G., Pedernana, M., and Gimeno Garcia, S.: Smart sampling and incremental function learning for very large high dimensional data, *Neural Networks*, 78, 75–87, <https://doi.org/10.1016/j.neunet.2015.09.001>, <http://dx.doi.org/10.1016/j.neunet.2015.09.001>, 2016.
- Malavelle, F. F., Haywood, J. M., Jones, A., Gettelman, A., Clarisse, L., Bauduin, S., Allan, R. P., Karset, I. H. H., Kristjánsson, J. E., Oreopoulos, L., Cho, N., Lee, D., Bellouin, N., Boucher, O., Grosvenor, D. P., Carslaw, K. S., Dhomse, S., Mann, G. W., Schmidt, A., Coe, H., Hartley, M. E., Dalvi, M., Hill, A. A., Johnson, B. T., Johnson, C. E., Knight, J. R., O'Connor, F. M., Partridge, D. G., Stier, P., Myhre, G., Platnick, S., Stephens, G. L., Takahashi, H., and Thordarson, T.: Strong constraints on aerosol-cloud interactions from volcanic eruptions, *Nature*, 546, 485–491, <https://doi.org/10.1038/nature22974>, 2017.
- McCormick, M. P., Thomason, L. W., and Trepte, C. R.: Atmospheric effects of the Mt Pinatubo eruption, *Nature*, 373, 399–404, <https://doi.org/10.1038/373399a0>, 1995.
- 10 Myles, L., Meyers, T. P., and Robinson, L.: Relaxed eddy accumulation measurements of ammonia, nitric acid, sulfur dioxide and particulate sulfate dry deposition near Tampa, FL, USA, *Environmental Research Letters*, 2, <https://doi.org/10.1088/1748-9326/2/3/034004>, 2011.
- Nowlan, C. R., Liu, X., Chance, K., Cai, Z., Kurosu, T. P., Lee, C., and Martin, R. V.: Retrievals of sulfur dioxide from the Global Ozone Monitoring Experiment 2 (GOME-2) using an optimal estimation approach: Algorithm and initial validation, *Journal of Geophysical Research: Atmospheres*, 116, n/a–n/a, <https://doi.org/10.1029/2011JD015808>, <http://dx.doi.org/10.1029/2011JD015808>, d18301, 2011.
- 15 Rix, M., Valks, P., Hao, N., Loyola, D., Schlager, H., Huntrieser, H., and Flemming, J. and Koehler, U. and Schumann, U. and Inness, A.: Volcanic SO₂, BrO and plume height estimations using GOME-2 satellite measurements during the eruption of Eyjafjallajökull in May 2010, *Journal of Geophysical Research (Atmospheres)*, 117, D00U19, <https://doi.org/10.1029/2011JD016718>, 2012.
- Robock, A.: Volcanic eruptions and climate, *Reviews of Geophysics*, 38, 191–219, <https://doi.org/10.1029/1998RG000054>, 2000.
- Spurr, R., de Haan, J., van Oss, R., and Vasilkov, A.: Discrete-ordinate radiative transfer in a stratified medium with first-order rotational Raman scattering, *Journal of Quantitative Spectroscopy & Radiative Transfer*, 109, 404–425, <https://doi.org/10.1016/j.jqsrt.2007.08.011>, 2008.
- 20 Theys, N., De Smedt, I., Yu, H., Danckaert, T., van Gent, J., Hörmann, C., Wagner, T., Hedelt, P., Bauer, H., Romahn, F., Pedernana, M., Loyola, D., and Van Roozendaal, M.: Sulfur dioxide retrievals from TROPOMI onboard Sentinel-5 Precursor: algorithm theoretical basis, *Atmospheric Measurement Techniques*, 10, 119–153, <https://doi.org/10.5194/amt-10-119-2017>, <http://www.atmos-meas-tech.net/10/119/2017/>, 2017.
- 25 von Glasow, R., Bobrowski, N., and Kern, C.: The effects of volcanic eruptions on atmospheric chemistry, *Chemical Geology*, 263, 131–142, <https://doi.org/10.1016/j.chemgeo.2008.08.020>, halogens in Volcanic Systems and Their Environmental Impacts, 2009.
- Xu, J., Schüssler, O., Loyola R., D., Romahn, F., and Doicu, A.: A novel ozone profile shape retrieval using Full-Physics Inverse Learning Machine (FP-ILM), *IEEE J. Sel. Topics Appl. Earth Observ. Remote Sens.*, 10, 5442–5457, <https://doi.org/10.1109/JSTARS.2017.2740168>, 2017.
- 30 Yang, K., Liu, X., Krotkov, N. A., Krueger, A. J., and Carn, S. A.: Estimating the altitude of volcanic sulfur dioxide plumes from space borne hyper-spectral UV measurements, *Geophysical Research Letters*, 36, <https://doi.org/10.1029/2009GL038025>, <http://dx.doi.org/10.1029/2009GL038025>, 2009.
- Yang, K., Liu, X., Bhartia, P. K., Krotkov, N. A., Carn, S. A., Hughes, E. J., Krueger, A. J., Spurr, R. J. D., and Trahan, S. G.: Direct retrieval of sulfur dioxide amount and altitude from spaceborne hyperspectral UV measurements: Theory and application, *Journal of Geophysical Research: Atmospheres*, 115, <https://doi.org/10.1029/2010JD013982>, <http://dx.doi.org/10.1029/2010JD013982>, 2010.
- 35

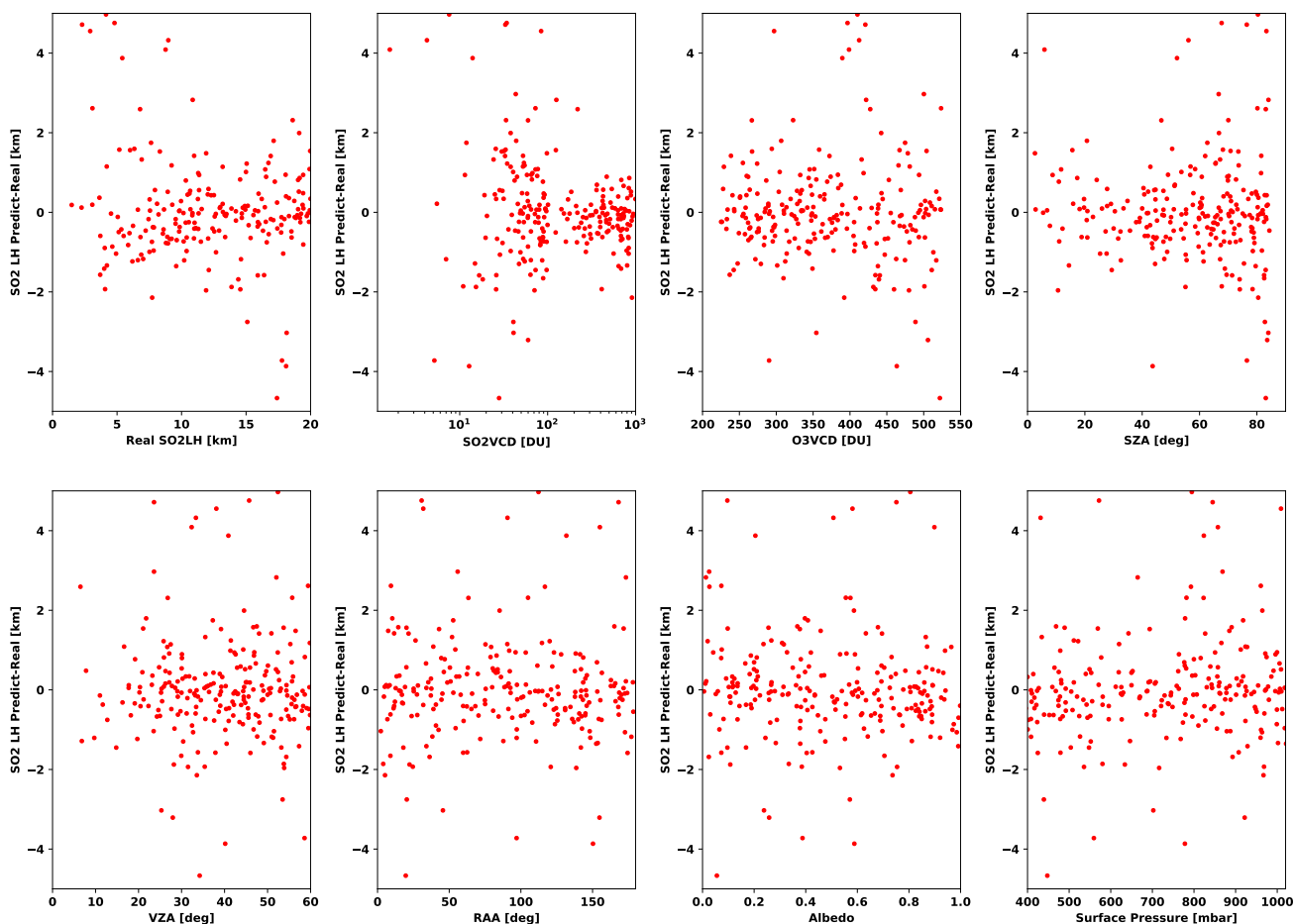


Figure 1. Dependency of the retrieved SO₂ layer height as a function of 8 parameters as indicated. Plotted are the layer height differences (in [km]) between retrieved layer heights and those simulated using the independent verification dataset (i.e. a 10% subdivision of the entire training dataset). For this plot we used the entire training data set, i.e. applied to optimization.

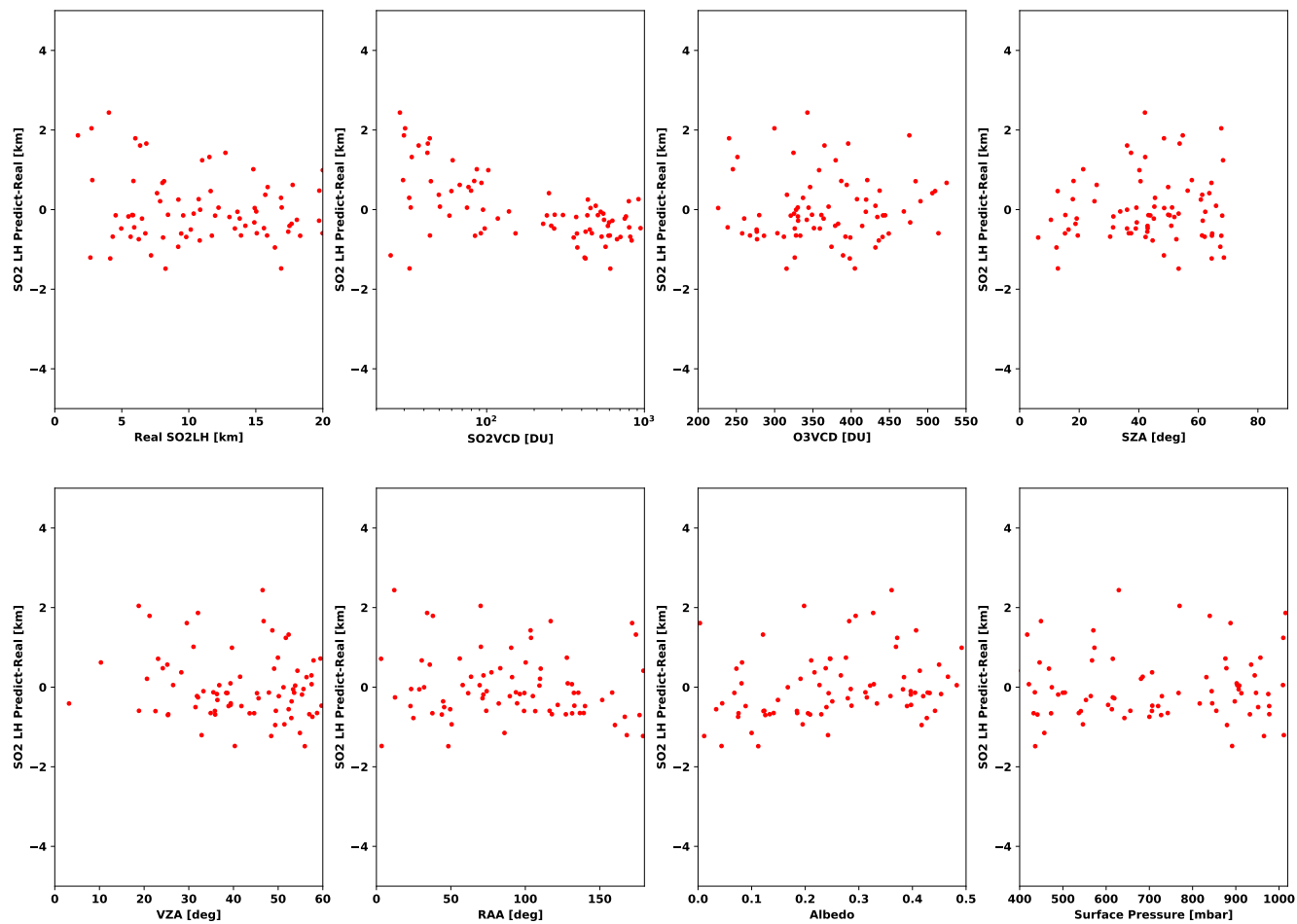


Figure 2. Same as Fig. 1 but with an optimized training dataset restricted to SO_2 VCD values >20 DU, SZAs $<75^\circ$ and albedos <0.5 .

Table 1. Physical parameters varied for the generation of reflectance spectra.

Parameter	Range
SZA	0–90°
VZA	0–60°
RAA	0–180°
Surface albedo	0–1
Surface height	0–8 km
O ₃ VCD	225–525 DU
SO ₂ VCD	0–1000 DU
SO ₂ LH	2.5–20 km

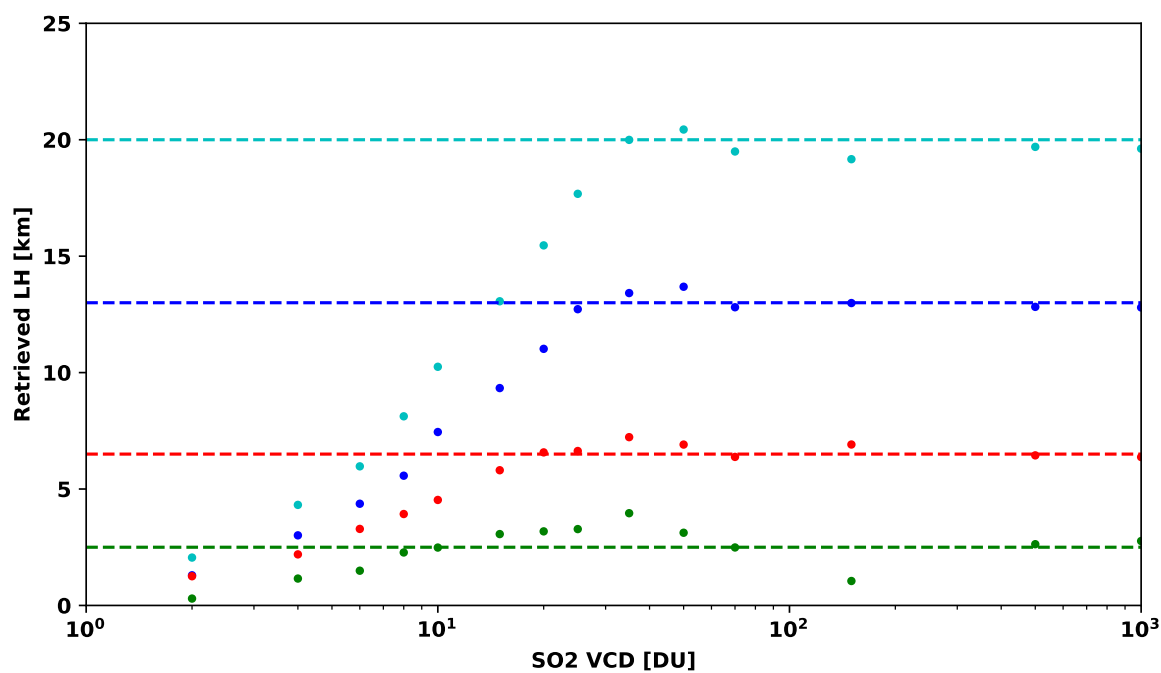


Figure 3. Dependency of the retrieved SO₂ LH as a function of SO₂ total vertical column, using an independent test dataset with O₃ =385 DU, SZA=30°, VZA=60°, RAA=30°, surface albedo 0.05, surface pressure 1013 mbar. Color coded are the different LHs for which the test spectra have been generated.

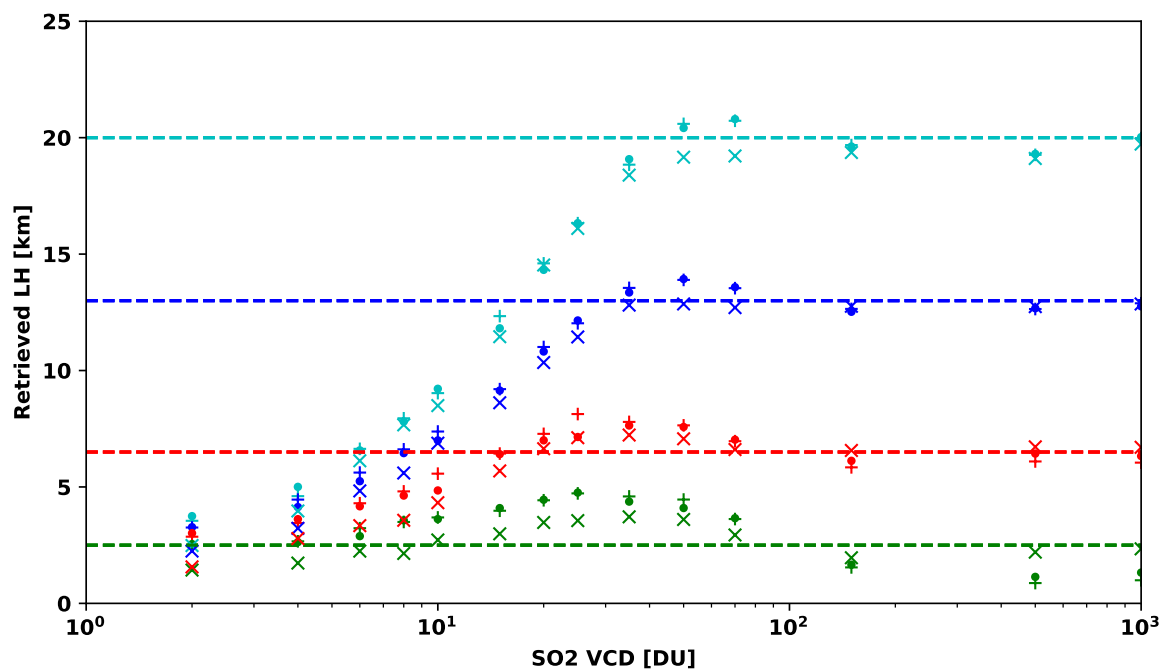


Figure 4. Dependency of the retrieved SO₂ LH on the SNR. Same as Fig. 3 but with three different SNR values: +: SNR=800, ●: SNR=1000, x:1200.

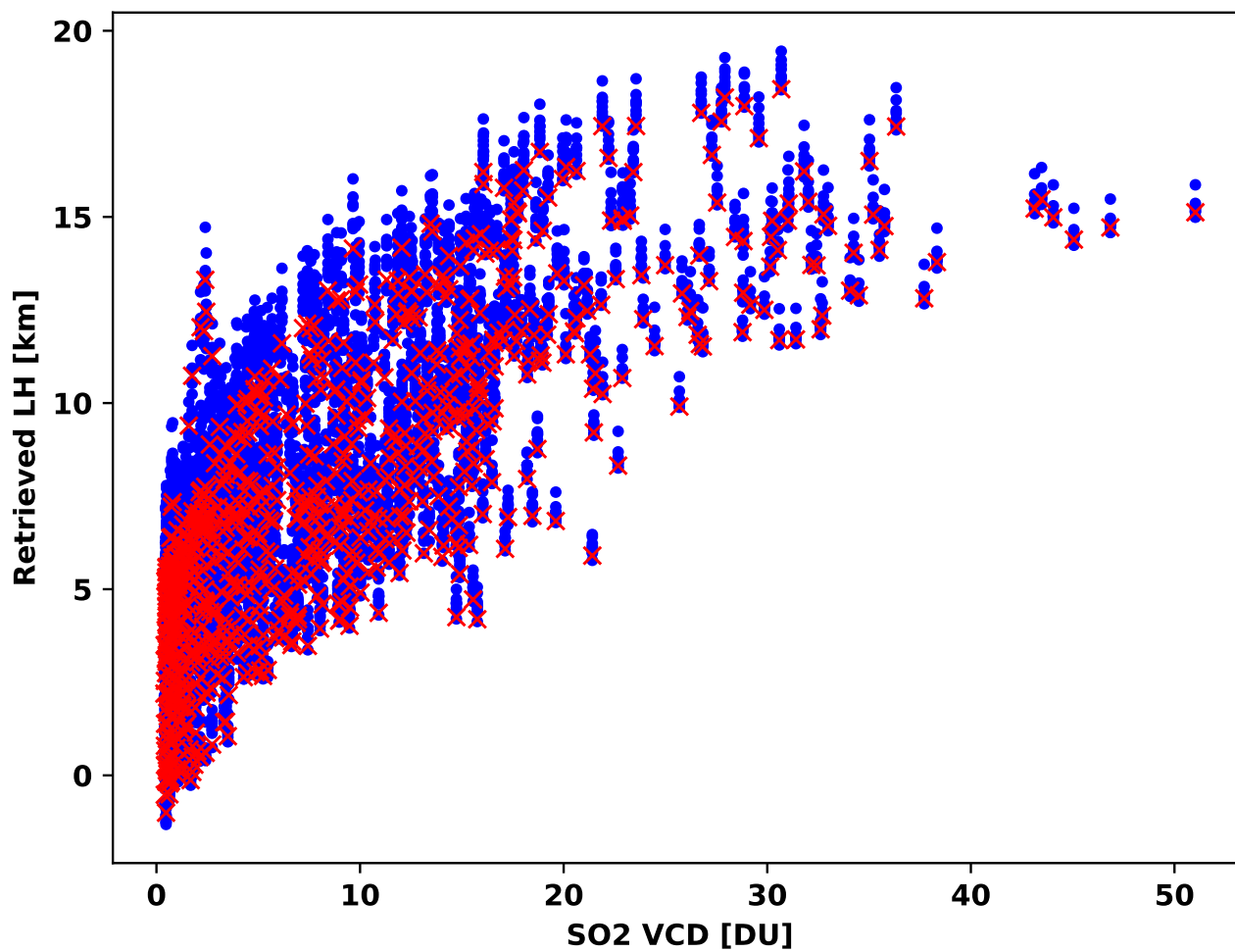


Figure 5. Dependency of the retrieved SO_2 LH on the instrument row. The SO_2 LH as a function of SO_2 VCD is shown for the Sinabung eruption. Blue dots show the SO_2 LH result for every 50th detector row, whereas red crosses show the LH interpolated to the measurement row.

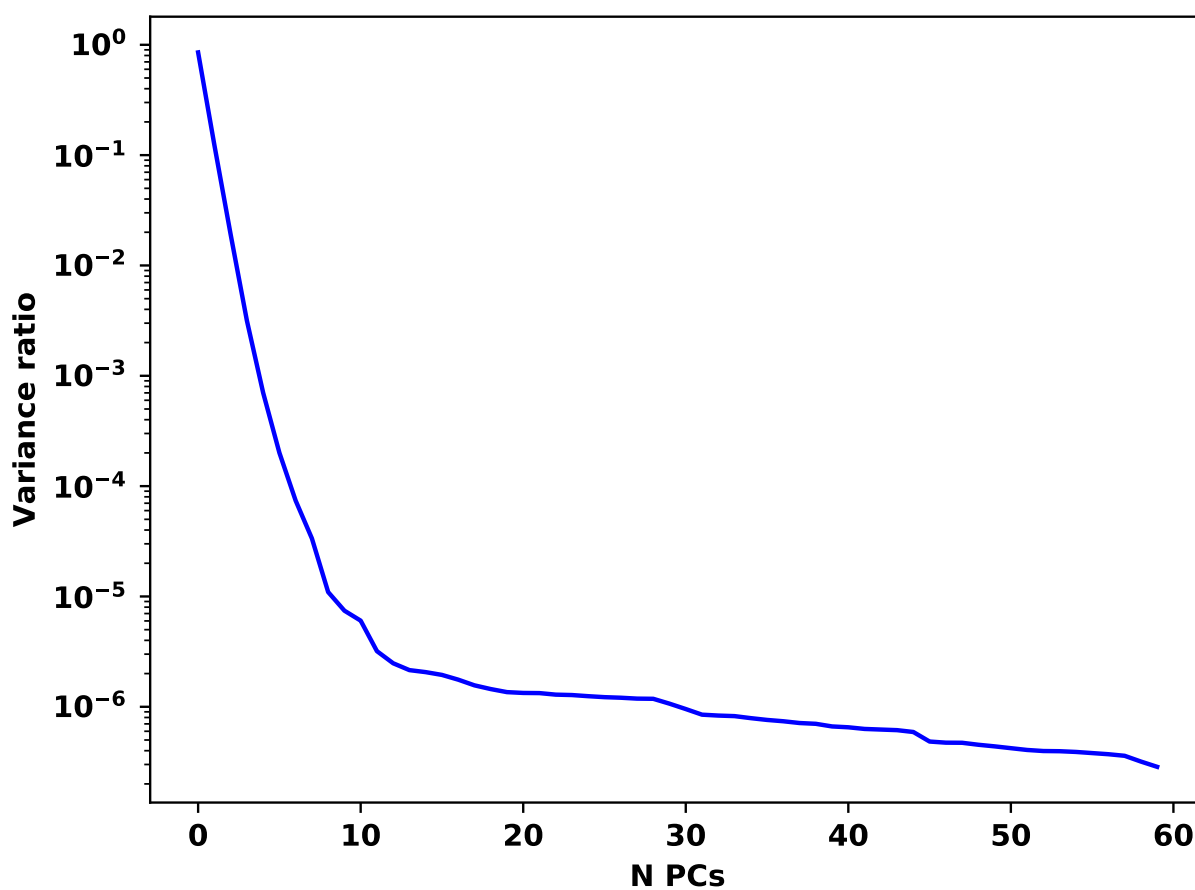


Figure 6. "Explained" variance ratio as a function of the number of principal components.

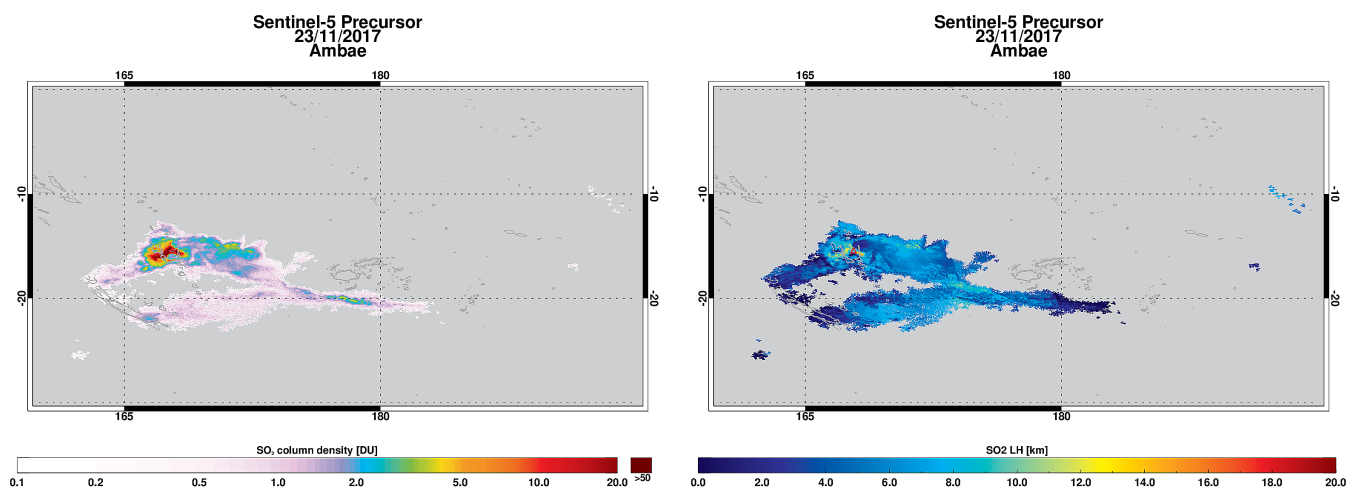


Figure 7. SO₂ VCD (left) and SO₂ LH (right) for the TROPOMI measurements of the Ambae volcano on 23 November 2017, at overpass time around 02:00h UTC.

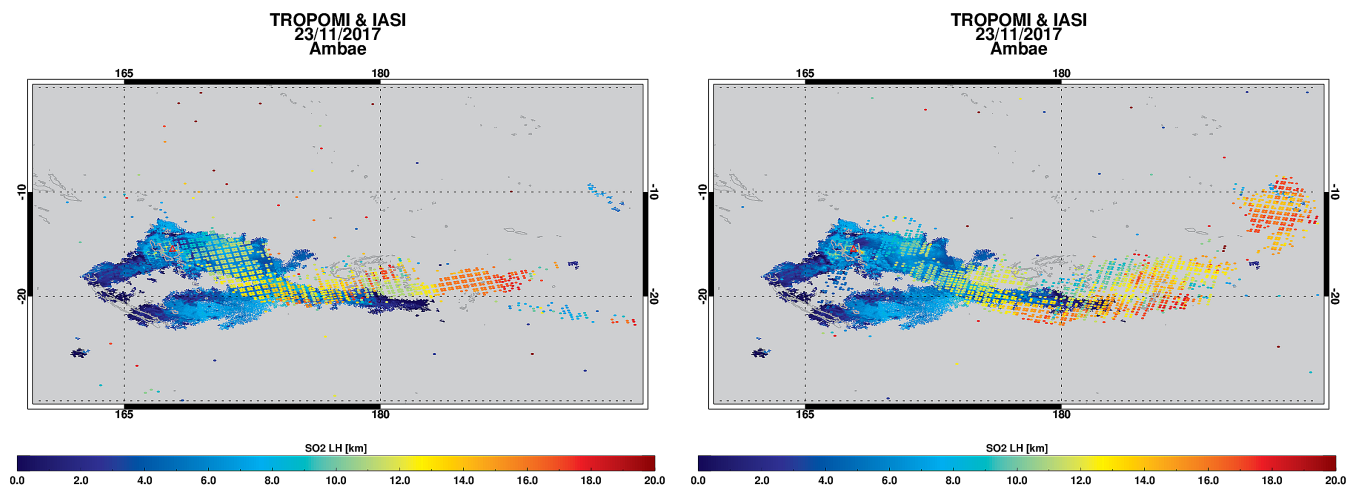


Figure 8. Comparison of S5p/TROPOMI SO₂ LH results with MetOp-A and -B/IASI SO₂ LH results for the Ambae SO₂ plume on 23 November 2017. The colored circles are the IASI results, with overpass times around 11:00h (left) and 21:15h UTC (right).

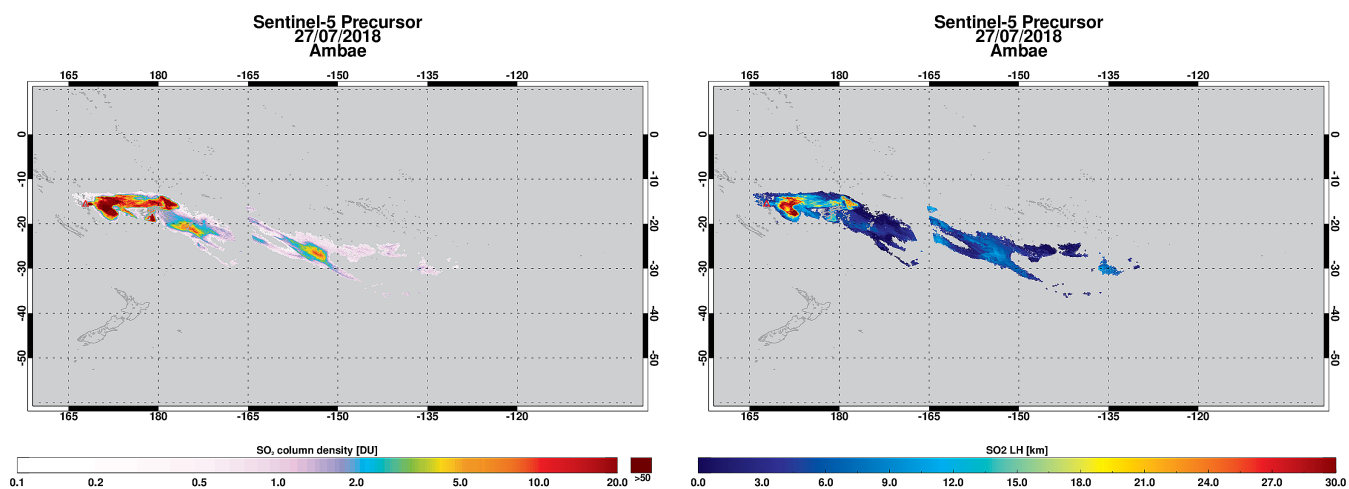


Figure 9. SO₂ VCD (left) and SO₂ LH (right) for the TROPOMI measurements of the Ambae volcano on 27 July 2018, at overpass time of around 02:00h UTC.

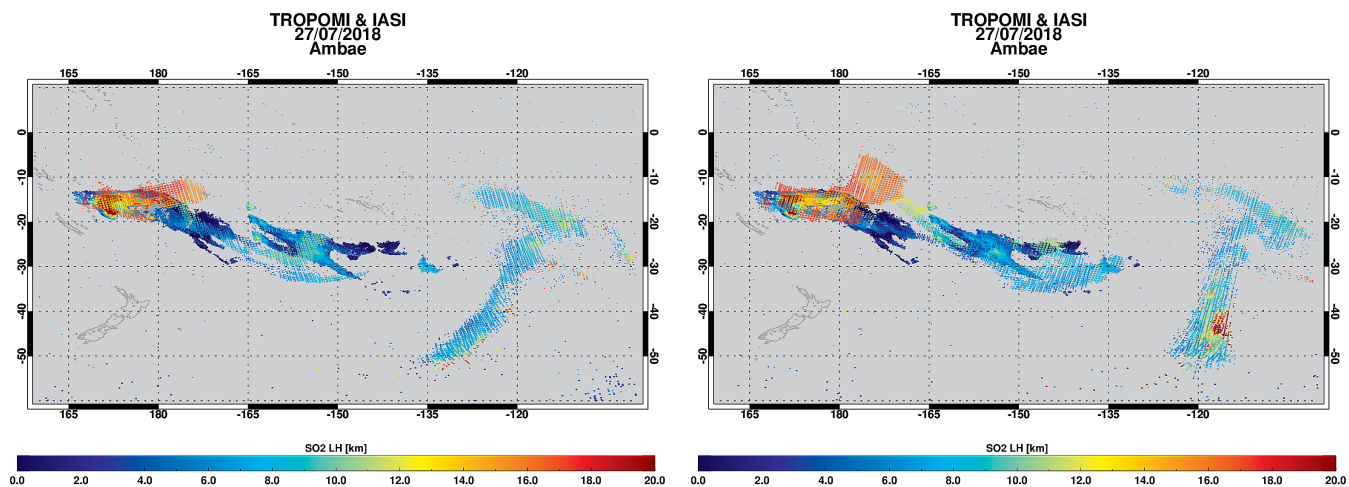


Figure 10. Comparison of S5p/TROPOMI SO₂ LH results with MetOp-A and -B IASI SO₂ LH results for the Ambae SO₂ plume on 27 July 2018. The colored circles are the IASI results with overpass times around 13:00h (left) and 23:00h UTC (right).

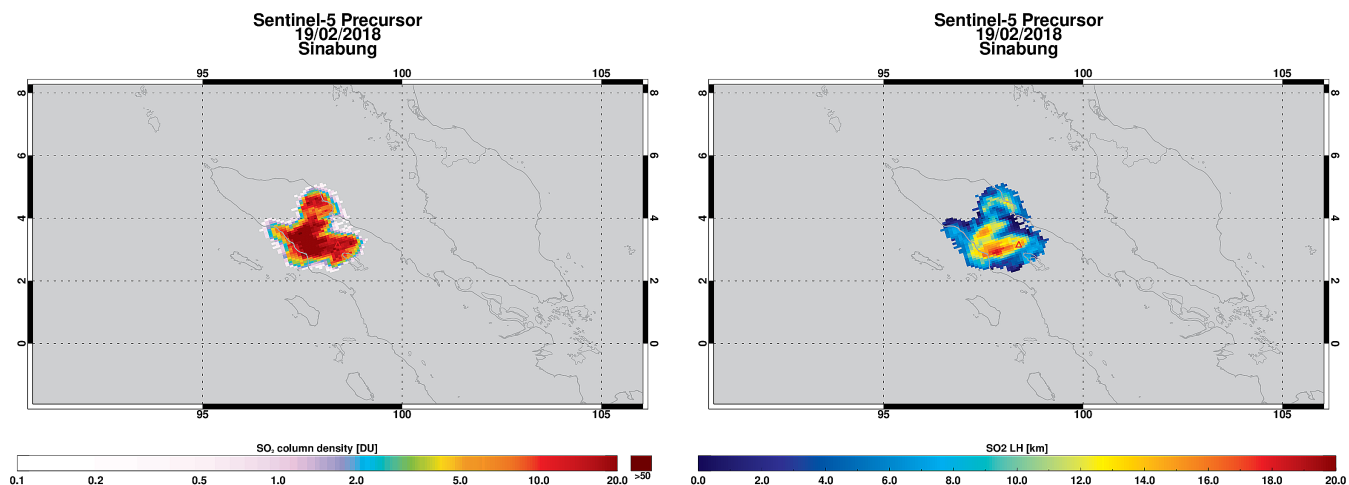


Figure 11. SO₂ VCD (left) and SO₂ LH (right) for the TROPOMI measurements of the Sinabung volcano on 19 February 2018, at overpass time around 06:30h UTC.

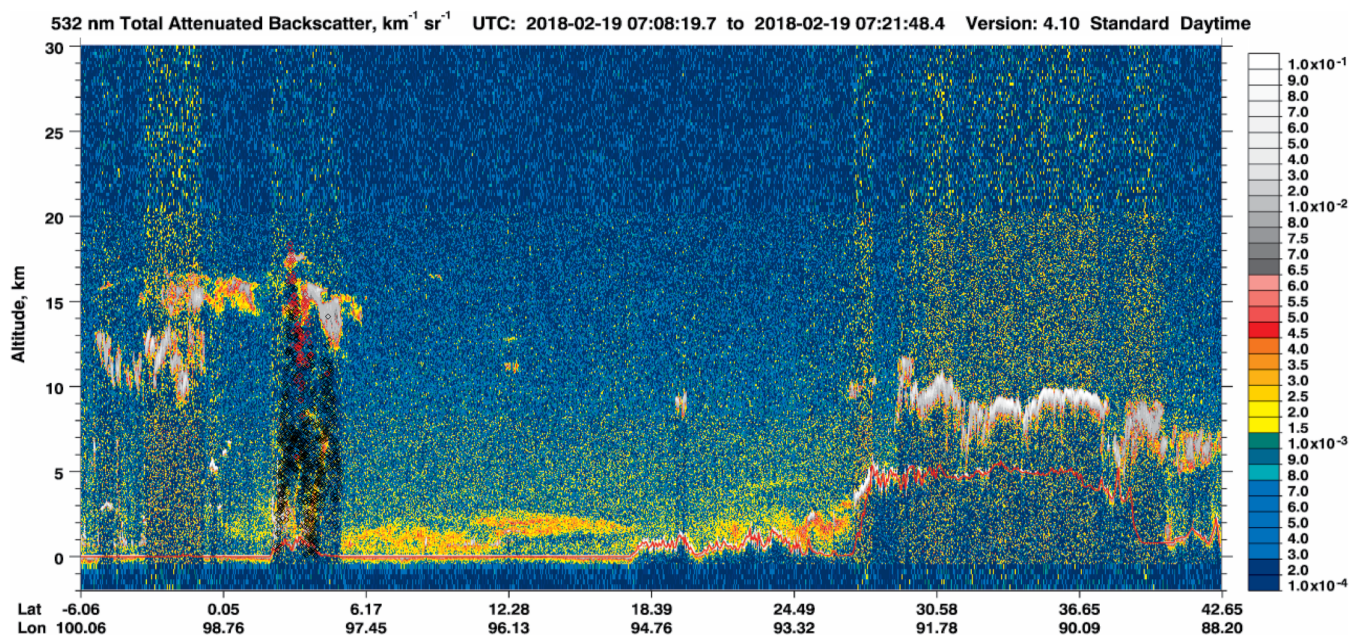


Figure 12. CALIOP/CALIPSO 532 nm total attenuated backscatter measurements (around 07:15h UTC) of the Sinabung volcanic eruption on 19 February 2018. Black diamonds are the FP_ILM SO₂ LH results. Red diamonds show the retrieved LH for pixels with SO₂ VCD > 20 DU, for which the uncertainty is less than 2 km. The volcano is located at 3.17N, 98.39E. The plume is clearly visible in the left part of the image. Image credit: NASA

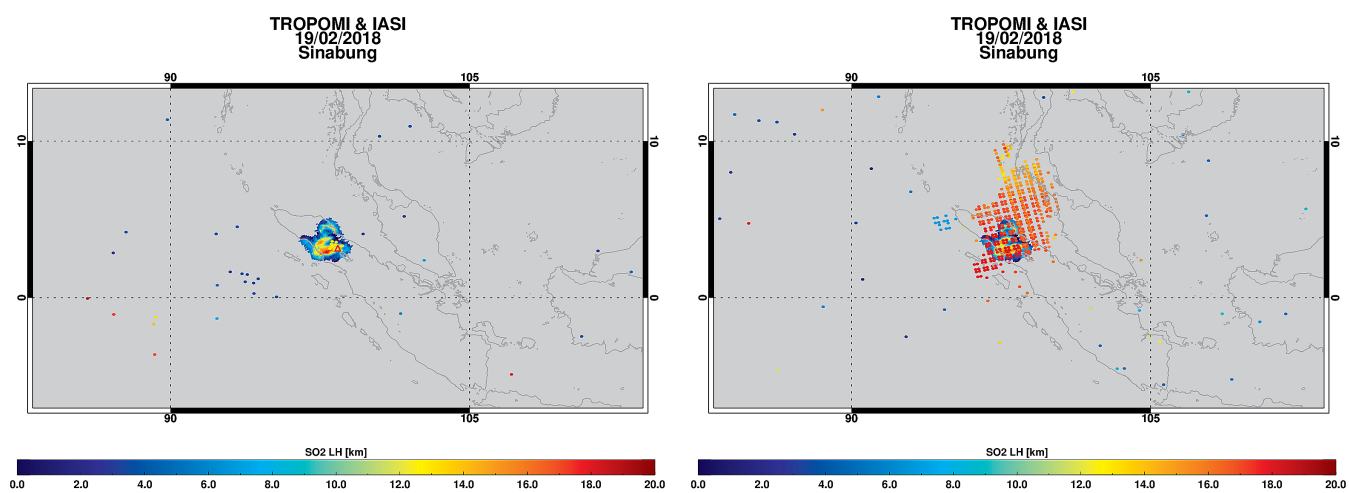


Figure 13. Comparison of S5p/TROPOMI SO₂ LH results with MetOp-A and -B IASI SO₂ LH results for the Sinabung SO₂ plume on 19 February 2018. The colored circles are the IASI results with overpass times at around 03:30 (left) and 15:00h UTC (right).

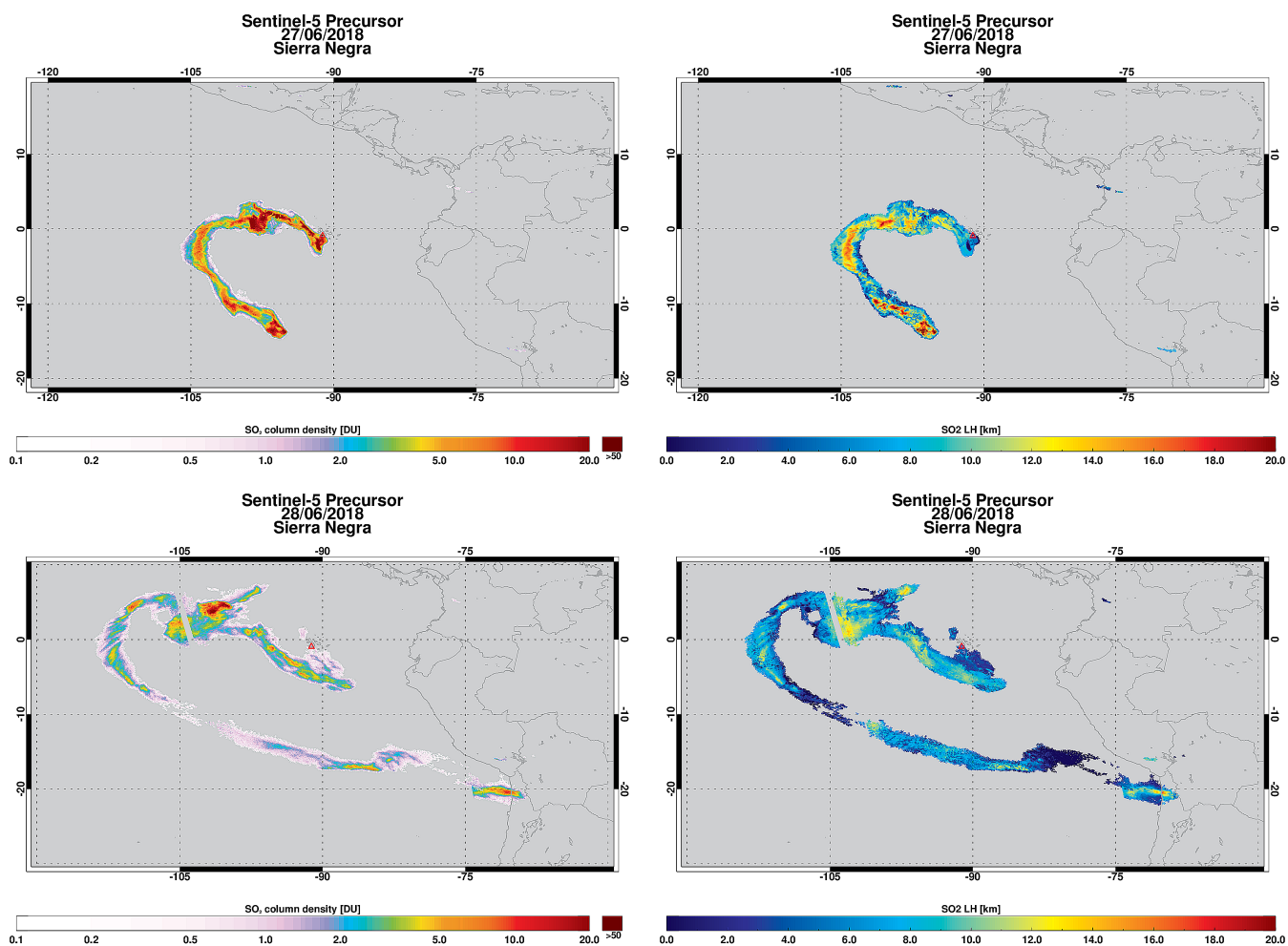


Figure 14. SO₂ VCD (left) and SO₂ LH (right) for the TROPOMI measurements of the Sierra Negra volcano on 27 (top) and 28 June 2018 (bottom), with overpass times around 19:50h UTC.

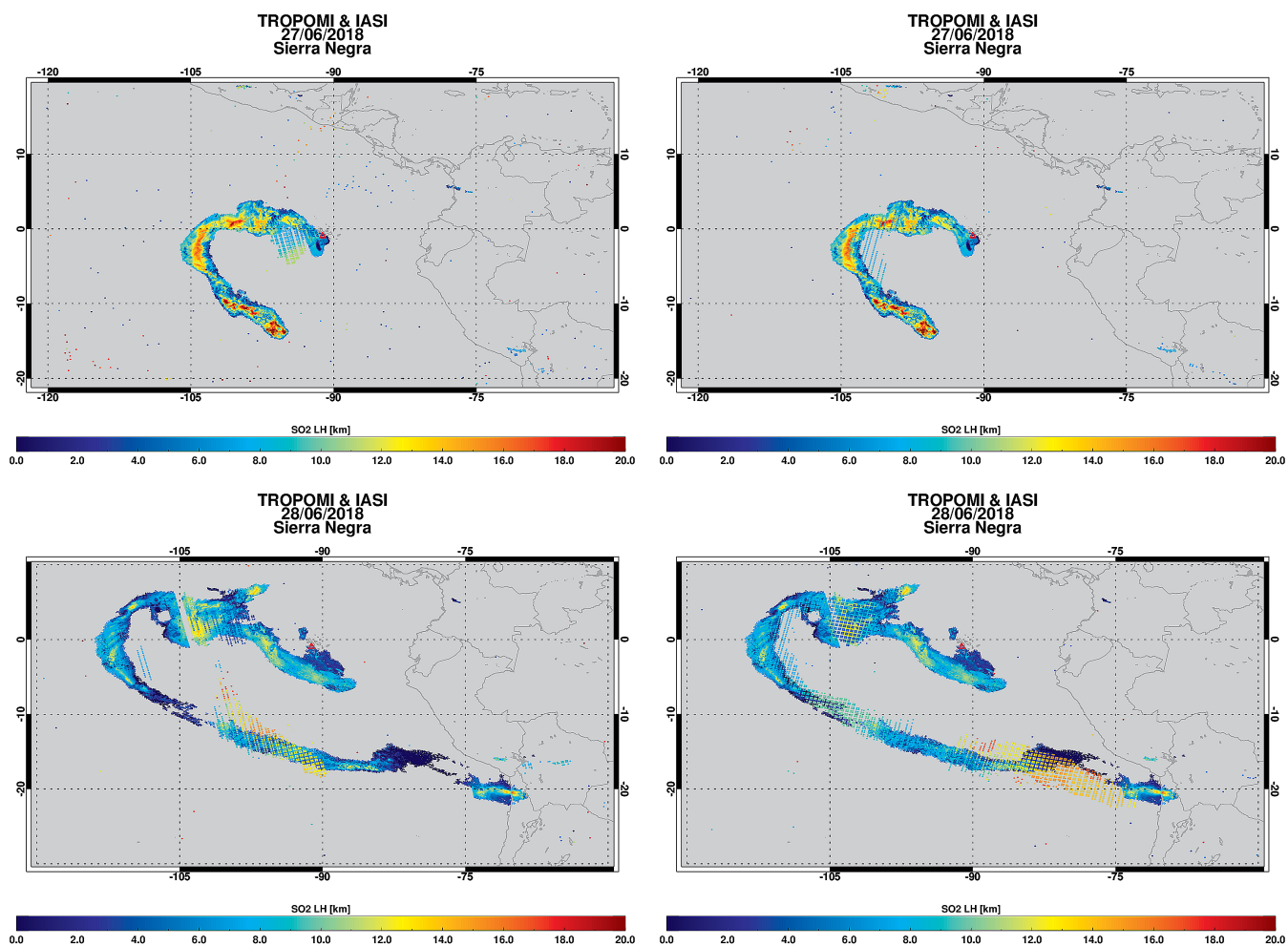


Figure 15. Comparison of S5p/TROPOMI SO₂ LH results with MetOp-A and -B IASI SO₂ LH results for the Sierra Negra SO₂ plume on 27 (top) and 28 June 2018 (bottom). The colored circles are the IASI results with overpass times around 02:00h (left) and 14:00h UTC (right).